

Mechanistic studies of fluorescent sensors for the detection of reactive oxygen species†

Belinda Heyne, Sara Ahmed and J. C. Scaiano*

Received 4th September 2007, Accepted 15th November 2007

First published as an Advance Article on the web 3rd December 2007

DOI: 10.1039/b713575k

Two new sensors for the detection of reactive oxygen species have been synthesized and characterized; they contain the 4-amino-7-nitrobenzofurazan (ABF) moiety covalently tethered to a phenol. Comparison of sensors ABFhd and dABFhd (the latter containing two *ortho*-methyl groups) shows that introduction of steric bulk leads to an improvement of fluorescent sensor performance, thus confirming our previous predictions based on computational chemistry. ABFhd and dABFhd are new tools for biological applications involving reactive oxygen species, in particular oxygen-centered radicals.

Introduction

During the past two decades, there has been a growing interest into the investigation of reactive oxygen species (ROS), which play a central, significant role in oxidative damage of biological systems.¹ ROS are derived from the metabolism of molecular oxygen and have been implicated in the aging process and in numerous diseases such as atherosclerosis, neurodegenerative diseases and cancer.^{2–7} ROS are known to react with a large variety of molecules including proteins, lipids, carbohydrates and nucleic acids. Targeted compounds, which are more reactive towards ROS, include unsaturated lipids, specific amino acids (sulfhydryl group) and aromatic compounds.² On the other hand, it is believed that different ROS can have characteristic roles and reactivities *in vivo*.²

It is therefore essential to develop accurate and sensitive methods for their detection. Fluorescent sensors have received much attention because of their sensitivity and their non-invasive nature. Good fluorescent sensors should be easy to synthesize, have a dark initial state (*i.e.*, non-fluorescent) and be fully compatible with the target media. For biological sensors, such compatibility must include absorbance in a convenient spectral region and minimal overlap of their fluorescence with cell autofluorescence.

In a recent study, we proposed a new sensor for the detection of ROS: NBFhd, which contains a fluorescent moiety, *N*-methyl-4-amino-7-nitrobenzofurazan (NBF), tethered to a phenolic structure that acts as a quencher and also as a hydrogen donor (Chart 1).⁸ While this new sensor proved to be efficient in the detection of a variety of ROS, it is also limited in the amount of fluorescent molecule that can be released (15% to 20% of the starting material). This result was linked to the mechanism of reaction of the sensor. It was proposed in the case of the interaction of NBFhd with peroxy radical that two radicals were required. The first radical was initiating the formation of an NBFhd phenoxy radical intermediate, which in turn reacted with a second peroxy radical and water. Only the attack of this second

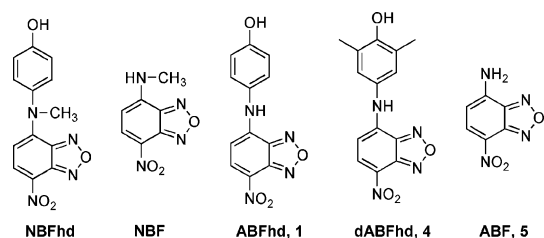


Chart 1 Structure of the different sensors and the fluorescent molecules they release upon exposure to ROS.

peroxy radical at the *para*-position was involved in the release of the fluorescent moiety NBF.⁸ A computational chemistry approach proved that favorable energetics for the formation of the *ortho*-coupling product served as a side reaction that does not involve NBF release. On the basis of computational studies it was suggested that introducing steric bulk, such as methyl groups at the *ortho*-positions, could lead to more *para*-coupling, and as a result may help to increase the amount of fluorescent moiety released.

Due to severe oxidation problems, the synthesis of a dimethyl *ortho*-substituted analogue of NBFhd proved to be extremely difficult. Therefore, in order to assess the prediction based on computational chemistry, a modified version of NBFhd, ABFhd **1** and its dimethyl analogue, dABFhd **4** were synthesized. As observed in Chart 1, the tertiary amine of the fluorescent sensor was substituted by a hydrogen in ABFhd **1**, instead of a methyl group.

Experimental

All chemicals were purchased from Aldrich and used as received. The ¹H NMR spectra were recorded on a Bruker-Avance-400 spectrometer at 400 MHz. Samples were prepared in methyl sulfoxide-*d*₆ (99%) purchased from Aldrich. The chemical shifts are quoted using the δ scale and the coupling constants are expressed in Hz. Mass spectra (see ESI†) were recorded on a Kratos-Concept-II instrument.

University of Ottawa, Department of Chemistry, 10 Marie Curie, Ottawa, ON, K1N 6N5, Canada. E-mail: tito@photo.chem.uottawa.ca

† Electronic supplementary information available: NMR spectra, Stern–Volmer plot, HPLC chromatogram, estimation of number of radicals, synthesis of quinoneimine. See DOI: 10.1039/b713575k

Synthesis of 4-(4-hydroxyphenylamino)-7-nitrobenzofurazan (ABFhd), 1

The synthesis of ABFhd was based on a procedure outlined in a previous study.⁸ Briefly, 610 mg of 4-chloro-7-nitrobenzofurazan (3.05 mmol) were dissolved in 5 ml methanol. Then, 500 mg of 4-aminophenol (4.58 mmol) were added. The mixture was refluxed at 75 °C under N₂ atmosphere. After 1 h, 769 mg of sodium bicarbonate (9.15 mmol) dissolved in 5 ml of Millipore water were added dropwise to the stirring solution. Upon cooling, dark brown–reddish crystals of the desired compound precipitated (760 mg, 2.79 mmol, 91.5% yield). ¹H NMR (DMSO-d₆, 298 K): δ = 6.45 (d, *J* = 9.12 Hz, 1H), 6.85 (d, *J* = 8.8 Hz, 2H), 7.23 (d, *J* = 8.8 Hz, 2H), 8.44 (d, *J* = 9.12 Hz, 1H), 9.73 (s, 1H), 10.7 (br s, 1H). The accurate mass was measured to be 272.0597 *m/z* for a structure C₁₂H₈N₄O₄.

Synthesis of 2,6-dimethyl-4-nitrosophenol, 2

The synthesis of **2** was based on a procedure outlined by Um *et al.*⁹ Briefly, 10 g of 2,6-dimethylphenol (81.9 mmol) were dissolved in a solution of 85 ml of 99% ethanol containing 2.54 ml of concentrated sulfuric acid, while kept below 0 °C. 6.42 g of sodium nitrite (93 mmol) dissolved in 15 ml of Millipore water were added dropwise to the stirring solution. A dark yellow precipitate formed immediately. The precipitate, 2,6-dimethyl-4-nitrosophenol **2**, was collected by filtration (9.0 g, 59.6 mmol, 72.8% yield). ¹H NMR(DMSO-d₆, 298 K); δ = 1.89 (d, *J* = 9.96 Hz, 6H), 7.09 (s, 1H), 7.51 (s, 1H). EI found: 151 *m/z*.

Synthesis of 2,6-dimethyl-4-aminophenol hydrochloride, 3

Following a literature procedure,¹⁰ 33 mg of 10% palladium on activated carbon were suspended in 4 ml of water. To the suspension was added 252 mg of NaBH₄ (6.6 mmol) dissolved in 5 ml of Millipore water. Then, a solution of 500 mg of **2** (3.3 mmol) dissolved in 20 ml of 2 M NaOH was added dropwise under N₂ to the stirring mixture. The mixture was refluxed under N₂ for 2 h. 3 ml of pure hydrochloric acid were added in order to destroy the excess NaBH₄ and to form the hydrochloride salt since 2,6-dimethyl-4-aminophenol is easily oxidized. The suspension was filtered and the filtrate was evaporated under vacuum to obtain a tan powder. The crude was used as obtained for the next step, synthesis of compound **4**. ¹H NMR (DMSO-d₆, 298 K): δ = 2.16 (s, 6H), 6.87 (s, 2H), 8.56 (s, 1H), 10.12 (s, 3H).

Synthesis of 4-(2,6-dimethyl-4-hydroxyphenylamino)-7-nitrobenzofurazan (dABFhd), 4

The synthesis of dABFhd **4** has not been reported before and was based on a procedure outlined in a previous study.⁸ Briefly, 372 mg of 4-chloro-7-nitrobenzofurazan (1.87 mmol) were dissolved in 20 ml methanol. Then, 500 mg of **3** (3.62 mmol) were added. The mixture was refluxed at 75 °C under N₂ atmosphere. After 2 h, 471 mg of sodium bicarbonate (5.6 mmol) dissolved in 5 ml of Millipore water were added dropwise to the stirring solution. Upon cooling, dark brown crystals of the desired compound precipitated (284.5 mg, 0.94 mmol, 50.3% yield). ¹H NMR (DMSO-d₆, 298 K): δ = 6.45 (d, *J* = 9.12 Hz, 1H), 6.85 (d, *J* = 8.8 Hz, 2H), 7.23 (d, *J* = 8.8 Hz, 2H), 8.44 (d, *J* = 9.12 Hz, 1H),

9.73 (s, 1H), 10.7 (br s, 1H). The accurate mass was measured to be 300.08479 *m/z* for a structure C₁₄H₁₂N₄O₄.

Synthesis of 4-amino-7-nitrobenzofurazan (ABF), 5

The fluorescent compound **5** was synthesized according to the literature.¹¹ The crude product was purified by column chromatography with 3 : 2 ethyl acetate : hexane elution, to afford pure **5** (98 mg, 0.544 mmol, 46.9% yield). ¹H NMR (DMSO-d₆, 298 K): δ = 6.35 (d, *J* = 9.0 Hz, 1H), 8.47 (d, *J* = 9.0 Hz, 1H), 8.85 (s, 2H). EI found: 180 *m/z*.

Spectroscopic measurements

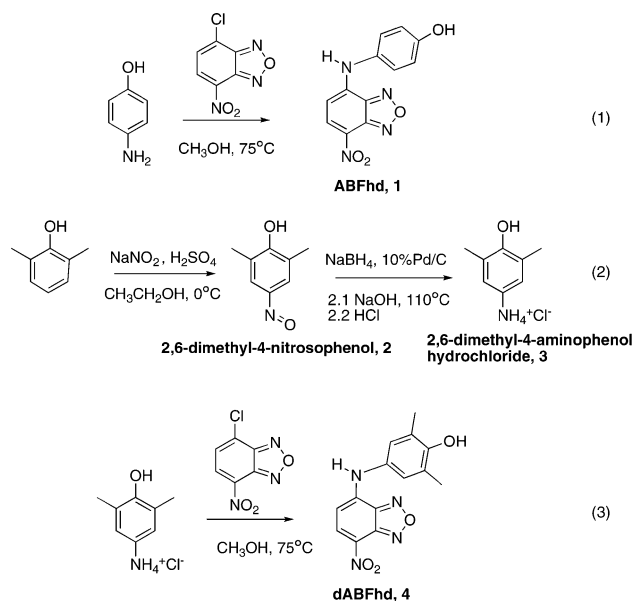
All the steady state emission spectra were recorded using a Photon Technology International spectrofluorimeter. The excitation wavelength for both ROS sensors was set up at 460 nm.

Lifetime fluorescence measurements were performed on a EasyLife LS (Photon Technology International). The excitation was performed with a 440 nm pulsed LED and the broadband emission was measured at 540 nm.

All absorption spectra were recorded on a Varian CARY-50 UV–vis spectrophotometer. All samples were placed in a spectro quality quartz cuvette, 1 cm path length.

Results and discussion

In phosphate buffer, 4-amino-7-nitrobenzofurazan (ABF **5**, Chart 1) and *N*-methyl-4-amino-7-nitrobenzofurazan (NBF, chart 1),¹² present similar photophysical properties with a relative quantum yield of 0.03 (compared to Rhodamine G6 at 22 °C). The fluorescent molecule ABF **5** fulfils our requirement for developing a fluorescent sensor. Indeed, with a fluorescence maximum around 540 nm, ABF will not interfere with cell autofluorescence.¹³ The synthesis of ABFhd **1** and its dimethyl *ortho*-substituted form (dABFhd **4**) is illustrated in Scheme 1. ¹H NMR spectra of ABFhd and dABFhd are consistent with the proposed structure and confirm the purity of the samples.



Scheme 1 Synthesis of ABFhd (**1**; eqn 1) and dABFhd (**4**; eqn 2 and 3).

The maximum absorption of ABFhd and dABFhd is occurring at 490 nm while the maximum of ABF is around 460 nm (Fig. 1). In addition, neither ABFhd nor dABFhd exhibit fluorescence within our detection limits. Both probes offer excellent contrast for the detection of ROS. As already shown for other fluorescent sensors,⁸ the absence of fluorescence for ABFhd and dABFhd can be rationalized on the basis of efficient electron transfer between the phenolic moiety and the excited chromophore. The rate constant for the fluorescence quenching of ABF by either phenol or 2,6-dimethylphenol was obtained from Stern–Volmer experiments (see ESI†). The fluorescence lifetime of ABF was measured to be 5.5 ns, which gives a measured rate constant of $4 \times 10^9 \text{ M}^{-1} \text{ s}^{-1}$ for quenching of ABF fluorescence by phenol and $5.6 \times 10^9 \text{ M}^{-1} \text{ s}^{-1}$ for quenching of ABF fluorescence by 2,6-dimethylphenol. These values are close to those found in a previous study.⁸ One should note that the methyl substitution of phenol at the *ortho*-position does not lead to a difference in the fluorescence quenching rate constant of excited ABF.

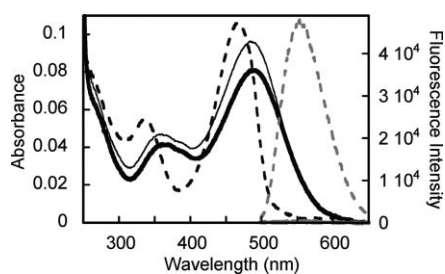


Fig. 1 Absorption (left) and fluorescence (right) spectra of ABFhd ($5 \times 10^{-6} \text{ M}$, thick line), dABFhd ($5 \times 10^{-6} \text{ M}$, thin line) and ABF ($5 \times 10^{-6} \text{ M}$, dashed line) in phosphate buffer pH 7.4. The excitation was set at 460 nm. Note: fluorescence spectra for ABFhd and dABFhd cannot be distinguished from the wavelength axis.

For concentrations ranging from $5 \times 10^{-7} \text{ M}$ to $2 \times 10^{-5} \text{ M}$ in phosphate buffer (PBS, 15 mM $\text{NaH}_2\text{P}_2\text{O}_4\text{-K}_2\text{HPO}_4$) with no more

than 1% of dimethylformamide; both fluorescence sensors obey the Beer–Lambert law, indicating the absence of self-association of both sensors in the ground state. The molar extinction coefficients were estimated at 490 nm to be $16\,420 \text{ M}^{-1} \text{ cm}^{-1}$ for ABFhd and $17\,300 \text{ M}^{-1} \text{ cm}^{-1}$ for dABFhd.

The ability of the two new fluorescence sensors to react with peroxy radical was analyzed in PBS by means of absorption and fluorescence spectroscopy. In both cases, peroxy radical was derived from the thermal decomposition of the water soluble 2,2'-azobis(2-amidinopropane) dihydrochloride (AAPH). AAPH is well known to decompose at 40°C yielding two carbon-centered radicals, which in turn react with molecular oxygen present in the solution to give two peroxy radicals.^{14,15} As observed in Fig. 2, the absorption peak corresponding to the probes decreases upon exposure to peroxy radical while the fluorescence spectra show the opposite behavior. In both cases, the increase of the fluorescence intensity over the reaction time was attributed to the release of the fluorescence compound ABF. The nature of the fluorescence compound release was attributed by HPLC with fluorescence detection (see ESI†). The decrease in absorption at *ca.* 490 nm probably incorporates some attack of peroxy radical at the chromophore.

Upon comparison of the change in fluorescence over time (Fig. 3b), both ABFhd and dABFhd experience the same small change during the first 30 minutes. After this point, dABFhd begins to evolve at an increasingly greater rate, and after 150 minutes (Fig. 3b), the fluorescence observed is almost double in the case of dABFhd compared to ABFhd. On the other hand, Fig. 3a shows a contrasting behavior for the evolution of the absorption peak of both sensors. Indeed, during the first 30 minutes the decrease in absorbance in the case of dABFhd is much more prominent, while after that period the decrease in absorbance occurs at similar rate for both sensors (Fig. 3a). The results obtained in Fig. 3b corroborate the prediction made by computational methods,⁸ that dABFhd should release a greater amount of ABF than ABFhd.

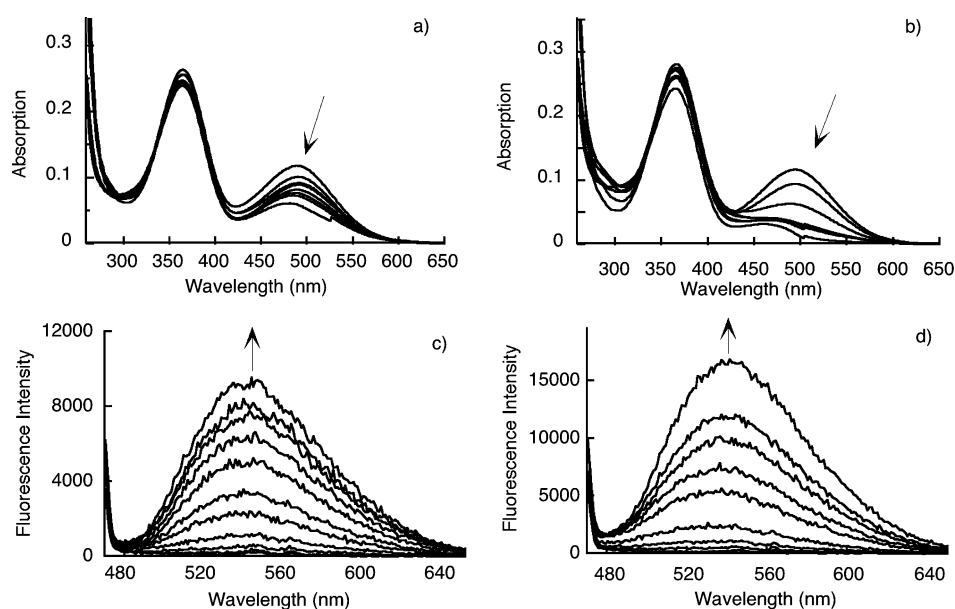


Fig. 2 Absorption and fluorescence emission spectra of a phosphate buffer solution pH 7.4 containing 10^{-2} M AAPH and $5 \times 10^{-6} \text{ M}$ ABFhd (a,c) or $5 \times 10^{-6} \text{ M}$ dABFhd (b,d), at 40°C under air.

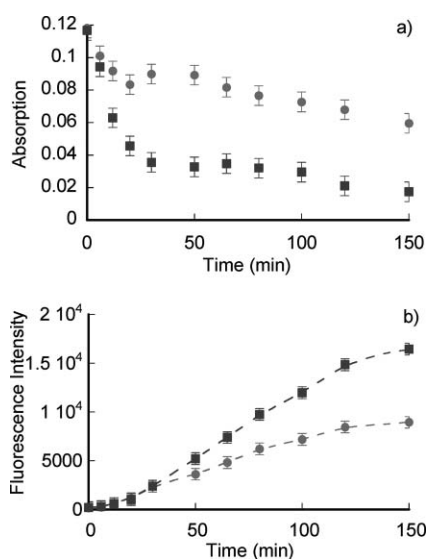
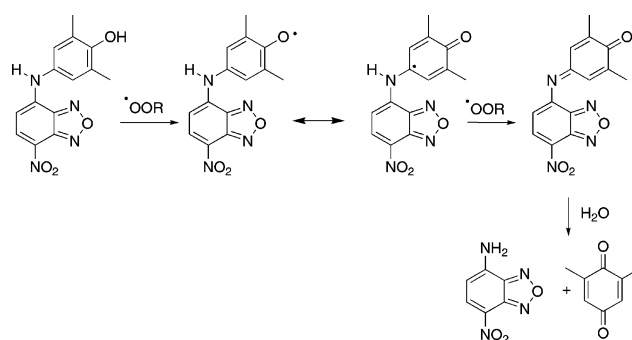


Fig. 3 Comparison of the maximum of (a) absorbance at 490 nm and (b) fluorescence emission at 540 nm of a phosphate buffer solution pH 7.4 containing 10^{-2} M AAPH and 5×10^{-6} M ABFhd (circle) or 5×10^{-6} M dABFhd (square), at 40 °C under air.

However, upon closer investigation it appears there are two phases inherent in the interaction of peroxy radical with both sensors before and after ~ 30 min. In the first phase there is an indication of a much faster consumption of the starting material in the case of dABFhd than ABFhd. This result is not surprising if one considers that the first step in the reaction mechanism involves the oxidation of the phenolic moiety. It is known that the rate constant for the reaction of 2,6-dimethylphenol with peroxy radical is higher than that for phenol.¹⁶ In the second phase, the consumption of the two sensors is similar with respect to the observed slow decrease in absorbance. On the other hand, the fluorescence intensity increases more rapidly in the case of the *ortho*-substituted sensor. Overall, these observations suggest that there is an intermediate step, which slows the release of ABF inherent in the mechanism of action for both sensors.

The characterization of the products resulting from the interaction of both sensors with peroxy radical was investigated by gas chromatography. The only products observed were 1,4-benzoquinone in the case of the ABFhd sensor and 2,6-dimethyl-1,4-benzoquinone in the case of dABFhd sensor (data not shown).

Even though the interaction of peroxy radical with the two new sensors ABFhd and dABFhd results in the release of a quinone and the fluorescence moiety ABF, our results suggest a mechanism of reaction different from that proposed for previously reported sensors of the same family.^{8,17} Indeed, as emphasized above, an intermediate step slowing the release of the fluorescent moiety is observed. Since the tertiary amine of ABFhd and dABFhd is substituted by a hydrogen instead of a methyl, a plausible mechanism could implicate the formation of a quinoneimine as an intermediate product in the reaction of both sensors with peroxy radical. As illustrated in Scheme 2, the first step of the reaction is probably a hydrogen atom transfer likely mediated by an electron transfer,^{8,17} from the phenolic moiety to the peroxy radical, leading to the formation of the corresponding phenoxyl radical. One might argue that the presence of the N–H bond in



Scheme 2 Mechanism proposed for the interaction of the new fluorescent sensors ABFhd and dABFhd with peroxy radical. The mechanism is similar for both sensors and only the case of dABFhd is illustrated here.

ABFhd and dABFhd can act also as a potential site of reactivity towards peroxy radicals. However, it seems unlikely that peroxy radicals will react initially with N–H rather than O–H. Indeed, it has been shown that for 4-hydroxydiphenylamine,¹⁸ a compound related to our sensors, that the bond dissociation energy of the N–H group is higher ($354.4 \text{ kJ mol}^{-1}$) than that of the OH moiety ($339.9 \text{ kJ mol}^{-1}$). Scheme 2 suggests that the phenoxyl radical derived from the sensor can react with a second peroxy radical (a pathway not available to NBFhd) to form the quinoneimine intermediate, which will then further slowly hydrolyze to give rise to the fluorescent moiety ABF and a quinone.

Further experiments allow us to confirm these hypotheses. Indeed, Fig. 4 shows that the bleaching of the sensor is almost totally prevented by Trolox, a water soluble analogue of vitamin E. This supports the occurrence of a process mediated by free peroxy radicals. In addition, the efficiency of ABFhd and dABFhd consumption was evaluated by comparing the consumption rate of the two sensors with the rate of the free radical production¹⁹ (see ESI†). From our experiments, it can be concluded that, on average, 2 peroxy radicals are scavenged by each sensor molecule consumed. Further, the fact that an equimolar concentration of Trolox almost totally suppresses the release of ABF suggests that the rate constant for radical attack on Trolox is significantly faster than that for sensors ABFhd and dABFhd.

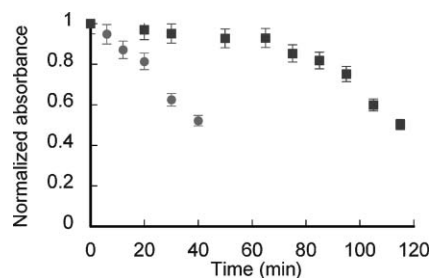


Fig. 4 Effect of the addition of 5×10^{-5} M Trolox on a phosphate buffer solution pH 7.4 containing 10^{-2} M AAPH and 5×10^{-5} M dABFhd under air at 40 °C. The circles represent the maximum absorbance of the sensor in the absence of Trolox and the squares in the presence of Trolox.

The nature of a quinoneimine as an intermediate product was indicated by the results shown in Fig. 5. Indeed, when Trolox is added to the solution after 30 minutes of reaction between peroxy radical and the sensors, the release of ABF by the sensor is quenched as illustrated in Fig. 5b, while the absorbance is restored

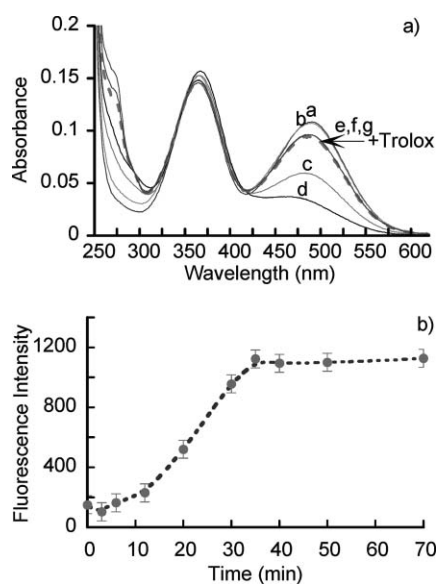


Fig. 5 Effect of the addition of 10^{-5} M Trolox after 35 min of reaction between 5×10^{-6} M ABFhd and peroxy radical produced by the thermal decomposition of 10^{-2} M AAPH in the presence of oxygen (air) at 40°C : (a) absorption spectrum ($t = 0$ min in a; $t = 6$ min in b; $t = 20$ min in c, $t = 35$ min in d; $t = 35$ min + Trolox in e; $t = 50$ min in f; $t = 70$ min in g), (b) fluorescence intensity at 540 nm.

(Fig. 5a). The quinoneimine intermediate formed during the first 30 minutes is reduced by the Trolox added to the solution giving back the starting material, which can account for the restoration of the absorbance while the fluorescence increase is blocked. To analyze the ability of the quinoneimine to slowly hydrolyze in buffer solution, we synthesized the molecule in organic solvent by reaction with lead dioxide (see ESI†). When dissolved in phosphate buffer solution pH 7.4, the quinoneimine hydrolyzed slowly to release the fluorescent compound ABF (data not shown). These results confirmed the mechanism of reaction proposed in Scheme 2.

Conclusion

In summary, we have developed two new sensors for the detection of ROS: ABFhd and dABFhd. Comparison of the two structures

shows that by introducing steric bulk such as *ortho*-methyl groups, the fluorescent sensor performance is improved since dABFhd is able to release more of the reporting fluorescent compound, ABF, than ABFhd, thus confirming our previous hypothesis based on computational chemistry. Thus, ABFhd and dABFhd are new tools to explore the involvement of reactive oxygen species, in particular oxygen-centered radicals, including superoxide, for biological applications.

Acknowledgements

This work was generously supported by funding from the Natural Sciences and Engineering Research Council of Canada, by the Canadian Foundation for Innovation and by the Government of Ontario. We would like also to thank Dr Keith U. Ingold for many helpful suggestions.

References

- 1 T. Kalai, E. Hideg, I. Vass and K. Hideg, *Free Radical Biol. Med.*, 1998, **24**, 649.
- 2 R. Colavitti and T. Finkel, *IUBMB Life*, 2006, **57**, 277.
- 3 B. Halliwell and J. M. C. Gutteridge, *Free Radicals in Biology and Medicine*, Oxford University Press, 1989.
- 4 D. Harman, *Age*, 1983, **6**, 86.
- 5 C. Hazelwood and M. J. Davies, *J. Chem. Soc., Perkin Trans. 2*, 1995, 895.
- 6 C. P. Schulze and R. T. Lee, *Curr. Atheroscl. Rep.*, 2005, **7**, 242.
- 7 G. Waris and H. Ahsan, *J. Carcinog.*, 2006, **5**, 14.
- 8 B. Heyne, C. Beddie and J. C. Scaiano, *Org. Biomol. Chem.*, 2007, **5**, 1454.
- 9 S. I. Um, J. K. Lee, Y. Kang and D. J. Baek, *Dyes Pigm.*, 2005, **65**, 93.
- 10 A. Vogel, *Vogel's Practical Organic Chemistry*, 4th edn, Longman Scientific & Technical, Essex, UK, 1978.
- 11 M. Boiocchi, L. Del Boca, D. Esteban-Gomez, L. Fabbrizzi, M. Licchelli and E. Monzani, *Chem.-Eur. J.*, 2005, **11**, 3097.
- 12 S. Uchiyama, T. Santa and K. Imai, *J. Chem. Soc., Perkin Trans. 2*, 1999, 2525.
- 13 J. E. Aubin, *J. Histochem. Cytochem.*, 1979, **27**, 36.
- 14 M. A. Cubillos, E. A. Lissi and E. B. Abuin, *Chem. Phys. Lipids*, 2000, **104**, 49.
- 15 G. S. Hammond and R. C. Neuman, Jr., *J. Am. Chem. Soc.*, 1963, **85**, 1501.
- 16 J. A. Howard and K. U. Ingold, *Can. J. Chem.*, 1963, **41**, 2800.
- 17 B. Heyne, V. Maurel and J. C. Scaiano, *Org. Biomol. Chem.*, 2006, **4**, 802.
- 18 V. T. Varlamov, *Russ. Chem. Bull., Int. Ed.*, 2004, **53**, 306.
- 19 E. Pino, A. M. Campos and E. Lissi, *Int. J. Chem. Kinet.*, 2003, **35**, 525.